Nuclear Technology

ISSN: 0029-5450 (Print) 1943-7471 (Online) Journal homepage: https://ans.tandfonline.com/loi/unct20

Empirical and Computational Pressure Drop Correlations for Pressurized Water Reactor Fuel Spacer Grids

Wang Kee In, Dong Seok Oh & Tae Hyun Chun

To cite this article: Wang Kee In, Dong Seok Oh & Tae Hyun Chun (2002) Empirical and Computational Pressure Drop Correlations for Pressurized Water Reactor Fuel Spacer Grids, Nuclear Technology, 139:1, 72-79, DOI: 10.13182/NT02-A3305

To link to this article: https://doi.org/10.13182/NT02-A3305

EMPIRICAL AND COMPUTATIONAL PRESSURE DROP CORRELATIONS FOR PRESSURIZED WATER REACTOR FUEL SPACER GRIDS

THERMAL HYDRAULICS

KEYWORDS: *correlation, pressure drop, spacer grid*

WANG KEE IN,* DONG SEOK OH, and TAE HYUN CHUN
Korea Atomic Energy Research Institute, P.O. Box 105, Yusong, Daejon, Korea, 305-600

Received May 31, 2001
Accepted for Publication November 24, 2001

Empirical and computational pressure drop correlations were developed to accurately estimate the pressure drop at the fuel spacer grid in a pressurized water reactor. The empirical correlation uses the balance of hydraulic forces acting on the spacer grid. The amount of pressure drop is assumed to depend largely on the reduction of the flow cross section, the flow constriction in the spacer region, and the frictional loss. The grid form drag due to the relative plugging and the flow constriction by the grid components were found to be the primary factors of the total pressure drop. The computational correlation combines the pressure drop due to flow blockage by the spacer grid and the pressure drop calculated by dynamics analysis. The pressure loss coefficients from the empirical correlation agree well with the measured ones for the spacer grids with and without the mixing vane. The computational correlation overpredicts the pressure loss coefficients for the spacer grid with the mixing vane.

I. INTRODUCTION

The amount of pressure drop at the fuel spacer grid is an important factor of the grid design because it influences the hydraulic performance of the existing fuel assembly and the capacity of the reactor coolant pump. Figure 1 illustrates a pressurized water reactor (PWR) fuel spacer grid with the mixing vane to increase departure from nucleate boiling performance. An excessive pressure loss in a fuel assembly would produce a large local cross flow that might cause the vibration of the fuel rods. The large pressure drop also requires a high head and power of the reactor coolant pump to provide the design coolant flow rate. Hence, an accurate prediction of the pressure drop at the spacer grid is necessary for the design of the reactor system and the advanced spacer design.

There are no reliable correlations for the pressure drop caused by the PWR fuel spacer, especially by the spacer with the mixing vane. De Stordeur[1] proposed pressure drop correlations for the fuel spacers with helical pins or the spacers used in gas-cooled breeder reactors. Since they were developed based on a limited amount of experimental data, the correlations given by de Stordeur are bound to be an approximation. Rehme[2] developed more precise correlations based on numerous experimental data for various fuel spacer configurations without the mixing vane. He assumed that the relative plugging by the fuel spacer straps and elements constitutes the main factor influencing the pressure loss. Kim et al.[3] developed an analytic pressure drop model for a PWR grid spacer without the mixing vane, which was not verified against the experimental data. Chun and Oh[4] also proposed a mechanistic model for the pressure drop at the spacer grids without and with a mixing vane. Their calculation uses the balance of hydraulic drag forces acting on the spacer elements such as grid strap, spring, dimple, and welding nugget. The drag coefficients of the spacer elements were taken from those of ideal configurations such as thin plate and small body protuberances. The additional pressure drop by the mixing vane is simply modeled by the vane-plugging area and the form drag coefficient for an abrupt flow blockage. The mechanistic model was known to underpredict the pressure loss coefficient of the fuel spacer and overpredict the pressure drop by the mixing vane.

The objective of this paper is to develop empirical and computational pressure drop correlations to estimate the pressure drop at the PWR fuel spacer grid. The empirical correlation modified the form drags on the grid

*E-mail: wkin@kaeri.re.kr

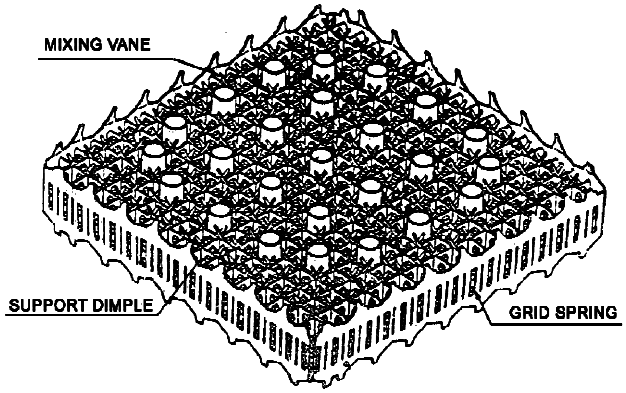

Fig. 1. Typical PWR fuel spacer grid with the mixing vane.

and the pressure drop caused by the mixing vane in the referenced mechanistic model. The individual form drag forces on the spacer elements are integrated into a total spacer form drag, and the form drag by the mixing vane is modeled to be consistent with the spacer form drag. The empirical correlation uses two empirical coefficients for the spacer grid and the mixing vane. The frictional drag coefficient of the grid strap is slightly modified for accurate prediction. The computational correlation is also proposed to estimate the spacer pressure drop using a computational fluid dynamics (CFD) analysis in which only the spacer strap and the mixing vane are modeled neglecting its thickness. The spacer loss coefficients from the correlations were compared with the experimental data available for two types of the fuel spacer grids.[5,6]

II. CORRELATION SETUP

II.A. Empirical Correlation

The empirical correlation is developed by modifying the mechanistic correlation[4] that uses the balance of drag forces acting on the spacer grid. The total drag force on the spacer grid without the mixing vane can be expressed by the sum of the form drag on the grid, the frictional drag on the grid strap, and the frictional drag on the rod (see Nomenclature on p. 78):

$$\sum F = F_{form,grid} + F_{fric.,grid} + F_{fric.,rod} \quad . \tag{1}$$

The pressure loss coefficient of the spacer grid without the mixing vane is generally defined as

$$C_{B,o} = \frac{\sum F}{\frac{\rho U_B^2}{2} A_o} \quad , \tag{2}$$

where ρ is the fluid density and U_B the bulk fluid velocity in the rod bundle; A_o is the nominal flow area.

By using the drag coefficient $C_{d,o}$, the form drag force on the grid in Eq. (1) can be written as

$$F_{form,grid} = C_{d,o} \frac{\rho U_S^2}{2} A_S \quad , \tag{3}$$

where U_S and A_S are the average fluid velocity at the spacer region and the projected grid cross section, respectively. The average fluid velocity at the spacer region is related to the bulk velocity by the continuity as

$$U_S = U_B \frac{A_o}{A_o - A_S} = U_B \frac{1}{1-\epsilon} \quad , \tag{4}$$

where ϵ $(= A_S/A_o)$ is the relative plugging of the flow cross section. Hence, the form drag force on the grid is written as

$$F_{form,grid} = C_{d,o} \frac{\rho U_B^2}{2} \frac{A_S}{(1-\epsilon)^2} \quad . \tag{5}$$

It should be noted that the form drag force in the mechanistic correlation was divided into four drag forces of the spacer elements, i.e., grid strap, spring, dimple, and welding nugget. The drag coefficients were simply taken from those of two-dimensional thin plate and small body protuberances. It is now simplified as a total form drag force on the grid using an empirical drag coefficient $C_{d,o}$.

Similarly, the frictional drag forces in Eq. (1) can be written by using the integrated drag coefficients:

$$F_{fric.,grid} = C_{d,grid}^{fric.} \frac{\rho U_B^2}{2} \frac{A_{grid}}{(1-\epsilon)^2} \tag{6}$$

and

$$F_{fric.,rod} = C_{d,rod}^{fric.} \frac{\rho U_B^2}{2} \frac{A_{rod}}{(1-\epsilon)^2} \quad , \tag{7}$$

where A_{grid} and A_{rod} indicate the wetted areas of the grid strap and the fuel rod at the spacer region, respectively. By substituting Eq. (2) and Eqs. (5), (6), and (7) into Eq. (1), the grid loss coefficient without the mixing vane is obtained as

$$C_{B,o} = C_{d,o} \frac{\epsilon}{(1-\epsilon)^2} + C_{d,grid}^{fric.} \frac{A_{grid}}{A_o} \frac{1}{(1-\epsilon)^2} + C_{d,rod}^{fric.} \frac{A_{rod}}{A_o} \frac{1}{(1-\epsilon)^2} \quad . \tag{8}$$

The integrated frictional drag coefficient of the grid strap is estimated by superposition of laminar drag and turbulent drag over a flat plate:

$$C_{d,grid}^{fric.} = C_{d,lam.}^{fric.} \frac{L_t}{H} + C_{d,tur.}^{fric.} \frac{H - L_t}{H} \quad , \tag{9}$$

where H and L_t are a grid height and a distance from the leading edge to the flow transition point, respectively. If

H is shorter than L_t, the second term on the right side of Eq. (9) vanishes. The transition Reynolds number on a flat plate is known to strongly depend on free stream turbulence.[7] Since turbulence upstream of the spacer grid in a fuel bundle was measured to be ~5% of the mean axial velocity,[6] the transition Reynolds number can be estimated as ~30 000 from which the flow transition length L_t is obtained. The integrated frictional drag coefficients for laminar and turbulent flows are obtained from the correlations for the flat plate,[7] respectively:

$$C_{d,\,lam.}^{fric.} = \frac{1.328}{\sqrt{\mathrm{Re}_L}} \quad , \tag{10}$$

and

$$C_{d,\,tur.}^{fric.} = \frac{0.523}{\ln^2 0.06\mathrm{Re}_L} \quad , \tag{11}$$

where Re_L is the Reynolds number based on the characteristic length of L_t or $H - L_t$.

The frictional drag coefficient of the fuel rod at the spacer region is estimated using the turbulent friction factor for a smooth round tube since pressure differentials are usually measured for the midgrids far downstream of the flow entrance; i.e.,

$$C_{d,\,rod}^{fric.} \frac{A_{rod}}{A_o} = C_{d,\,rod}^{fric.} \frac{4H}{D_h} = f \frac{H}{D_h} \quad , \tag{12}$$

where f and D_h are the Darcy friction factor and the hydraulic diameter, respectively. The McAdams correlation for the Darcy friction factor is used in this study; i.e.,

$$f = 0.184\mathrm{Re}_D^{-0.2} \quad . \tag{13}$$

The Reynolds number in Eq. (13) uses the hydraulic diameter as a characteristic length.

The grid loss coefficient C_B with the mixing vane is formulated by superposition of the grid loss coefficient without the mixing vane $C_{B,o}$ and that for the mixing vane $C_{B,mv}$:

$$C_B = C_{B,o} + C_{B,\,mv} \quad . \tag{14}$$

The effect of the mixing vane on the pressure drop in the mechanistic correlation was simply formulated by multiplication of an ideal form drag coefficient for abrupt flow blockage and a relative plugging of the flow cross section by the mixing vane. It is assumed in this study that the pressure drop by the mixing vane largely depends on the plugging of the flow cross section. Hence, similar to the form loss coefficient of the spacer grid, the pressure loss coefficient of the mixing vane can be modeled as

$$C_{B,\,mv} = C_{d,\,mv} \frac{\epsilon_{mv}}{(1 - \epsilon_{mv})^2} \quad , \tag{15}$$

where $C_{d,mv}$ and ϵ_{mv} $(= A_{mv}/A_o)$ are an empirical form drag coefficient for the mixing vane and a ratio of the plugging area of the mixing vane to the undisturbed flow area, respectively.

II.B. Computational Correlation

To maximize the benefit of the mixing vanes, their size, shape, bend angle, and location must be optimized. It is therefore essential to evaluate the turbulent flow characteristics in detail for the optimal design of the grid spacer with flow mixing promoters. Since the optimal spacer design should consider a large number of shapes and sizes of mixing vanes on the grid spacer, the utilization of the CFD method is valuable to select among alternate fuel spacer designs. Reference 8 reported that the CFD method could be quite useful for the optimal design of an advanced mixing vane based on a numerical study of flow mixing in a nuclear fuel assembly with the mixing vane on the spacer grid.

A single subchannel of one grid span is modeled using flow symmetry by a CFD code, CFX (Ref. 9). The spacer and mixing vanes are treated as infinite thin surfaces. Figure 2 shows the CFD models of the spacer grids with the mixing vane. The other fuel spacer elements such as the spring and arches are neglected for simplicity because their effect on the flow mixing is judged to be minimal only inside and near the spacer. The split-vane model with a vane cutout consists of 176 structured blocks with ~243 000 cells and another CFD model with no vane cutout of 180 blocks with ~247 000 cells. A fine grid was used near the spacer grid and the

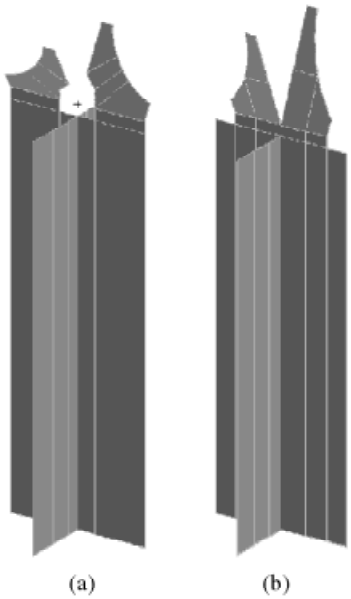

Fig. 2. CFD models of split-vane grids: (a) with vane cutout and (b) with no vane cutout.

rod surfaces. Details on the computational grids are described in a previous CFD study.[8]

The standard $k-\epsilon$ turbulence model of Launder and Spalding[10] was used in this calculation since it is practically useful for the complex turbulent flow in a nuclear fuel assembly. The standard underrelaxation method and hybrid difference scheme were used to obtain a converged solution. The calculation was terminated when the residual for the mass equation (sum of the absolute values of the net mass flux into or out of every cell in the flow field) is $<0.02\%$ of the total inlet mass flow rate. The pressure drop calculated by the CFD analysis is not accurate because the thickness of the spacer and the mixing vanes, and the spacer elements are neglected. Figure 3 shows the pressure distributions that were obtained from a CFD analysis. It shows a large pressure drop across the spacer grid that is caused primarily by the mixing vane blockage and the friction with the spacer grid and the fuel rod.

A computational correlation is proposed to estimate the pressure drop at the spacer grid with the mixing vane using the pressure drop predicted by the simplified CFD method. The CFD analysis does not include the effect of plugging of the flow cross section by the grid strap and the spacer elements on the pressure drop. Hence, the total pressure loss coefficient can be estimated from the CFD pressure drop and the form drag on the grid due to the relative plugging by the grid strap and the spacer elements:

$$C_B = \frac{\Delta P_{grid,\mathrm{CFD}}}{\frac{\rho U_B^2}{2}} + C_{d,o}\,\frac{\epsilon}{(1-\epsilon)^2} \quad . \tag{16}$$

III. RESULTS AND DISCUSSION

III.A. Correlation Constants

Kwon et al.[5] and Yang and Chung[6] presented the measured pressure loss coefficients at the PWR spacer grids with the mixing vane obtained from the hydraulic experiments for a 5×5 rod bundle. Kwon et al.[5] also provide the loss coefficients at the spacer grid without the mixing vane (tests 1 and 2). Table I summarizes the design features of the spacer grids and the mixing vanes used in those experiments. It is noted that the mixing vanes used in the experiments are the split-vane designs, with vane cutout (spacer 1) used by Kwon et al. and with no vane cutout (spacer 2) used by Yang and Chung.

The drag coefficient of the mixing vane ($C_{d,mv}$) in Eq. (15) can be determined using the measured loss coefficients for spacer 1 with and without the mixing vane. For spacer 2, only the measured loss coefficient with the mixing vane is available. Since the mixing vane for spacer 2 is similar to that for spacer 1, the form drag coefficient of the mixing vane for spacer 2 was assumed to be the same as that for spacer 1. The form drag coefficient of the spacer grid $C_{d,o}$ in Eq. (8) was then determined by a least-squares error fitting of the measured loss coefficients for spacers 1 and 2 without the mixing vane. Since the measured loss coefficient for spacer 2 without the mixing vane is not available, it was calculated by subtracting the loss coefficient of the mixing vane [Eq. (15)] from the loss coefficient for spacer 2 with the mixing vane.

Figure 4 shows the comparison of the form drag coefficients for spacers 1 and 2. The spacer drag coefficients appear to decrease as the Reynolds number increases. The drag coefficient for spacer 2 is slightly smaller than that for spacer 1 and tends to decrease rapidly as the Reynolds number increases. It can be seen that the measured drag coefficients are within $\pm 15\%$ of a best fit as follows:

$$C_{d,o} = 2.75 - 0.27 \log_{10}(\mathrm{Re}_B) \quad . \tag{17}$$

It is noted that the form drag coefficient of the spacer grid in Eq. (17) is also used in the computational correlation.

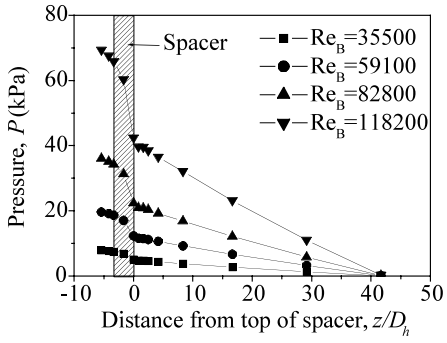

Fig. 3. Pressure distributions across spacer 1 by the CFD analysis.

TABLE I

Design Features of the Spacer Grids Used in this Study

Parameter	Spacer 1 (Ref. 5)	Spacer 2 (Ref. 6)
Rod diameter, d (mm)	9.5	9.5
Rod bundle pitch, p/d	1.353	1.326
Grid strap height, H (mm)	38.1	40.0
Strap thickness, t (mm)	0.46	0.45
Relative plugging of spacer elements, ϵ	0.23	0.23
Relative plugging of mixing vane, ϵ_{mv}	0.13	0.16
Mixing vane	Split vane with vane cutout	Split vane with no vane cutout

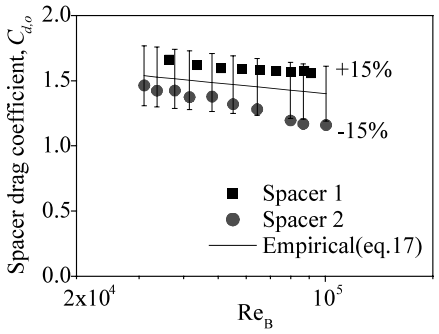

Fig. 4. Form drag coefficients of the spacers.

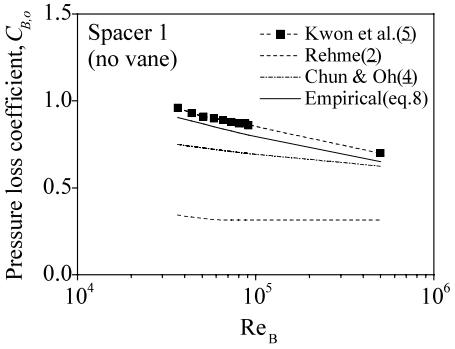

Fig. 6. Pressure loss coefficient for spacer 1 without the mixing vane.

Figure 5 shows the form drag coefficient of the mixing vane for spacer 1. It does not show noticeable dependency on the Reynolds number but rather a small variation in the range of 0.6 to 0.8. The proper value was assumed to its mean value, i.e.,

$$C_{d,mv} = 0.72 \quad . \tag{18}$$

III.B. Pressure Loss Coefficients

The pressure loss coefficients estimated by the correlations are compared with the measured data for spacer 1 (Ref. 5) and spacer 2 (Ref. 6), respectively. Since the measurements provided the spacer loss coefficients for a Reynolds number $<100\,000$, the measured data were extrapolated to a Reynolds number of 500 000, which is a nominal PWR operating condition. A power fit of the data was made to extrapolate to a Reynolds number of 500 000.

Figure 6 compares the loss coefficients for spacer 1 without the mixing vane. The Rehme correlation resulted in much lower loss coefficient than the measured value because the correlation coefficient was determined from the loss coefficient of a short and simply supported spacer. The mechanistic correlation proposed by Chun and Oh[4] also appears to underpredict the loss coefficient by 20%. This is because the mechanistic correlation uses the form drag coefficients of the spacer elements that are taken from those of simple geometric configurations. It can be seen in Fig. 6 that the empirical correlation slightly underpredicts the measured loss coefficient with a maximum error of 10%. The loss coefficient by the empirical correlation also shows good agreement with the measured one extrapolated to the Reynolds number of 500 000.

The pressure loss coefficients for the mixing vane (split vane with vane cutout) of spacer 1 are compared in Fig. 7, which shows a small variation independent of the Reynolds number. The measured loss coefficient is estimated to be 0.124 ± 0.025. Since the form drag coefficient of the mixing vane in the empirical correlation was determined as the mean value of the experimental data, the empirical loss coefficient is equal to 0.124. However, the mechanistic correlation by Chun and Oh[4] shows a somewhat higher loss coefficient of 0.151 due to the use of the form drag coefficient for sudden flow blockage. The computational correlation cannot separately estimate the loss coefficient of the mixing vane because the

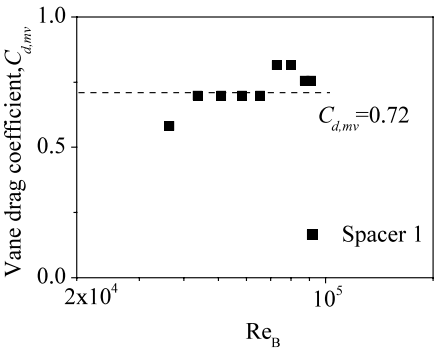

Fig. 5. Mixing vane drag coefficient for spacer 1.

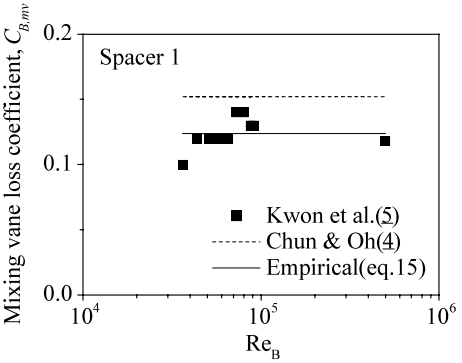

Fig. 7. Pressure loss coefficient of the mixing vane for spacer 1.

CFD calculation includes the pressure drops not only by the mixing vane but also by the grid and rod frictional loss in the spacer region.

Figure 8 shows the pressure loss coefficients for spacer 1 with the mixing vane (split vane with vane cutout). The mechanistic correlation[4] underpredicts the loss coefficient by 15% while the empirical correlation shows good agreement with the measurement within the error of 10%. It should be noted that the mechanistic correlation overpredicts the vane loss compared with the measured one by 22% as shown in Fig. 7. The computational correlation based on a simplified CFD analysis predicts the loss coefficient higher than the measured one by as much as 25% at low Reynolds numbers. The CFD model tends to show better agreement as the Reynolds number increases. The overprediction by the computational correlation seems to be caused by the fact that current CFD analysis neglected the spacer elements possibly perturbing the flow upstream of the mixing vane. In other words, the simplified CFD analysis appears to overly calculate the pressure drop by the mixing vane because the small body protuberances were neglected. Although the computational correlation predicts a somewhat larger pressure drop for the spacer with the mixing vane, it is useful to approximate the pressure drop across the fuel spacer grid with various designs of the mixing vane from a simplified CFD analysis.

Figure 9 shows the pressure loss coefficients for spacer 2 with the mixing vane (split vane with no vane cutout). The mechanistic correlation underpredicts the loss coefficient by as much as 15% at low Reynolds numbers. The empirical and computational correlations predict the loss coefficient higher than the measured one by a maximum of 8 and 17%, respectively. The slight overprediction by the empirical correlation is due to the use of the empirical spacer drag coefficient, which is higher than the measured one for spacer 2 as shown in Fig. 4. Similar to spacer 1, the larger pressure drop calculated by the simple CFD analysis resulted in overpredicting the loss coefficient for spacer 2 by the computational correlation. The correlation loss coefficients at the Reynolds number of 500 000 are somewhat larger than the extrapolated measurement.

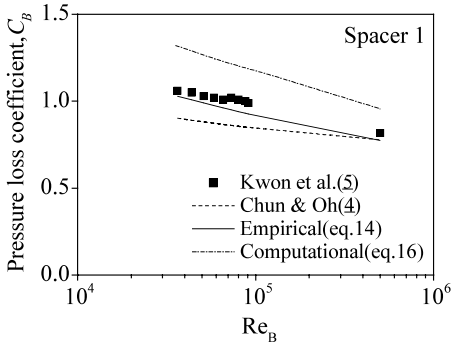

Fig. 8. Pressure loss coefficient for spacer 1 with the mixing vane.

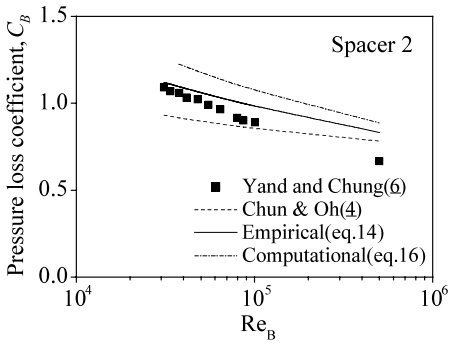

Fig. 9. Pressure loss coefficient for spacer 2 with the mixing vane.

Figure 10 is the graphic view of the pressure loss components for spacer 1 and spacer 2. The pressure drop at the spacer largely depends on the grid form loss due to the flow blockage by the grid strap and the spacer elements. The grid form loss is ~58 and 54% of the total pressure loss for spacer 1 and spacer 2, respectively. The frictional loss by the grid is in the range of 17 to 19% of the total loss for both spacers. The rod friction is slightly smaller than the grid friction. The form loss by the mixing vane is 13 and 16% for spacer 1 and spacer 2, respectively. The larger vane effect for spacer 2 is primarily due to the larger relative plugging of the mixing vane than for spacer 1.

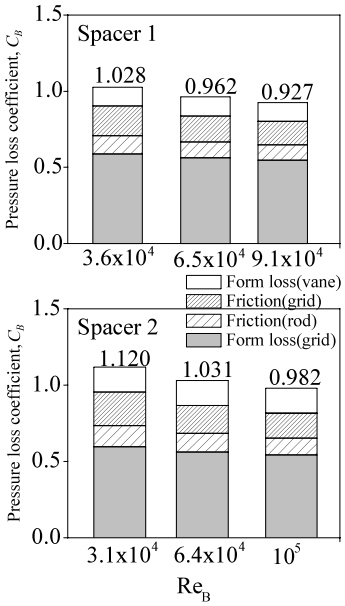

Fig. 10. Comparisons of pressure loss components.

IV. CONCLUSION

This study developed the empirical and computational pressure drop correlations for a PWR fuel spacer grid and compared the predictions with the measurements for two spacer grids. The empirical correlation uses the balance of drag forces acting on the spacer grid and the superposition of drag force caused by the mixing vane. The empirical drag coefficients for the spacer grid and the mixing vane were respectively determined using the available experimental data. The computational correlation is to estimate the pressure drop across the spacer grid with the mixing vane using the pressure drop calculated by a simplified CFD analysis. The grid pressure drop was represented by superposition of the CFD pressure drop and the pressure drop due to the relative plugging by the grid strap and the spacer elements.

The empirical correlation resulted in the pressure loss coefficients for the spacer grids with and without the mixing vane that agree with the experimental data well. The computational correlation predicted the loss coefficient of the spacer grid with the mixing vane to be higher than the measured one by as much as 25% at low Reynolds numbers and showed better agreement as the Reynolds number increases. Analysis of the grid pressure loss showed that the pressure drop at the spacer grid is primarily caused by the grid form loss due to the relative plugging by the grid strap and the spacer elements. The form loss by the mixing vane appears to be ~15% of the grid loss. It is therefore concluded that the new correlations would be useful in developing an advanced PWR fuel spacer by providing accurate estimation and analysis of the pressure drop at the spacer grid. However, in order to confirm the applicability of the new correlations in the spacer development and more accurately predict the pressure drop, the empirical drag coefficients need to be further verified and modified using a geometry correction factor with experimental data for various designs of the spacer grids in the future.

NOMENCLATURE

A_o = nominal flow area of rod bundle (m^2)

A_S = projected cross section of spacer grid (m^2)

A_{grid} = wetted area of the grid strap (m^2)

A_{rod} = wetted area of the fuel rod (m^2)

C = pressure loss coefficient

C_d = drag coefficient

f = Darcy friction factor

H = grid strap height (m)

L_t = flow transition length (m)

Re_B = Reynolds number based on hydraulic diameter of rod bundle

Re_D = Reynolds number based on characteristic hydraulic diameter

Re_L = Reynolds number based on characteristic length

U_B = bulk fluid velocity in a rod bundle (m/s)

U_S = average fluid velocity at the spacer region (m/s)

Greek

ρ = fluid density (kg/m^3)

ϵ = relative plugging of flow area

ACKNOWLEDGMENT

The authors express their appreciation to the Ministry of Science and Technology of Korea for financial support.

REFERENCES

1. A. N. DE STORDEUR, "Drag Coefficients for Fuel Element Spacers," *Nucleonics*, **19**, *6*, 74 (1961).

2. K. REHME, "Pressure Drop Correlations for Fuel Element Spacers," *Nucl. Technol.*, **17**, 15 (1973).

3. N. H. KIM, S. K. LEE, and K. S. MOON, "Elementary Model to Predict the Pressure Loss Across a Spacer Grid Without a Mixing Vane," *Nucl. Technol.*, **98**, 349 (1992).

4. T. H. CHUN and D. S. OH, "A Pressure Drop Model for Spacer Grids with and Without Flow Mixing Vanes," *J. Nucl. Sci. Technol.*, **35**, *7*, 508 (1998).

5. J. T. KWON, J. S. LIM, Y. H. KIM, K. T. KIM, and C. O. PARK, "Scoping Testing for the KAFD Mid Grid Proposals," *Proc. Annual KNS Spring Mtg.*, Cheju, Korea, May 23–25, 2001, Korea Nuclear Society (2001).

6. S. K. YANG and M. K. CHUNG, "Spacer Grid Effects on Turbulent Flow in Rod Bundles," *J. Korean Nucl. Soc.*, **28**, *1*, 56 (1996).

7. F. M. WHITE, *Viscous Fluid Flow*, pp. 261–267, 433–436, 500–502, McGraw Hill Book Company, New York (1974).

8. W. K. IN, "Numerical Study of Coolant Mixing Caused by the Flow Deflectors in a Nuclear Fuel Bundle," *Nucl. Technol.*, **134**, 187 (2001).

9. CFX INTERNATIONAL, "*CFX-4.2: Solver*," AEA Technology, Oxfordshire, United Kingdom (1997).

10. B. E. LAUNDER and D. B. SPALDING, "The Numerical Computation of Turbulent Flows," *Comput. Methods Appl. Mech. Eng.*, **3**, 269 (1974).

Wang Kee In [BS, 1984, and MS, 1986, mechanical engineering, Yonsei University, Korea; PhD, mechanical engineering, Korea Advanced Institute of Science and Technology (KAIST), 1998] is a principal engineer at the Korea Atomic Energy Research Institute working in the area of pressurized water reactor (PWR) thermal-hydraulic analysis. His background includes computational fluid dynamics analysis of turbulent flow in a PWR fuel assembly and multiphase flow analysis.

Dong Seok Oh (BS, 1983, and MS, 1985, mechanical engineering, Yeungnam University, Korea) is a senior engineer at the Korea Atomic Energy Research Institute (KAERI) working in the area of PWR thermal-hydraulic analysis. His background includes experimental study of turbulent flow in a PWR fuel assembly.

Tae Hyun Chun (BS, mechanical engineering, Ajou University, Korea, 1981; MS, 1985, and PhD, 1999, mechanical engineering, KAIST) is a principal engineer at KAERI. His background includes thermal-hydraulic analysis of a PWR core and critical heat flux analysis.